

Interface electron structure of Fe₃Al/TiC composites

PANG Lai-xue(庞来学)¹, SUN Kang-ning(孙康宁)^{1,2}, SUN Jia-tao(孙家涛)¹,
FAN Run-hua(范润华)^{1,2}, REN Shuai(任帅)¹

1. Key Laboratory of Engineering Ceramic of Shandong Province, Ji'nan 250061, China
2. Key Laboratory of Liquid Structure and Heredity of Materials, Ministry of Education, Shandong University, Ji'nan 250061, China

Received 29 June 2005; accepted 31 October 2005

Abstract: Based on YU's solids and molecules empirical electron theory (EET), interface valence electron structure of TiC-Fe₃Al composites was set up, and the valence electron density of different atomic states TiC and Fe₃Al composites in various planes was determined. The results indicate that the electron density of (100)_{Fe₃Al} is consistent with that of (110)_{TiC} in the first-class approximation, the absolute value of minimum electron density difference along the interface is 0.007 37 nm⁻², and the relative value is 0.759%. (110)_{TiC}//(100)_{Fe₃Al} preferred orientation is believed to benefit the formation of the cuboidal shape TiC. In the other hand, it shows that the particle growth is accompanied by the transport of electron, the deviation continuity of electron density intrinsically hinders the grain growth. The electron density of (100)_{TiC} is not consistent with Fe₃Al arbitrary crystallographic plane, thus it well explains that the increased titanium and carbon contents do not increase the size of large particles. The crystallographic orientation of (110)_{TiC}//(100)_{Fe₃Al} will improve the mechanical properties. Therefore interface electron theory is an effective theoretical implement for designing excellent property of composites.

Key words: TiC/Fe₃Al composite; intermetallic matrix composites; ceramic particles; YU's theory; interface; electron density

1 Introduction

Recently a few studies[1–3] have been carried out to utilize carbides or borides as reinforcements in iron aluminides, thus improving their mechanical properties. Additionally, an intermetallic matrix reinforced with ceramic phase might make it possible to overcome some of the problems that prevent the use of monolithic intermetallic alloys[4]. Among them titanium carbide with high hardness, low density and low chemical reactivity was found to be a suitable reinforcement for wear and high temperature application.

The nature of the interface between reinforcement and matrix plays a very important role in determining the properties. Differences in atomic structure, chemical ingredients, atom bonding manners between the matrix and the reinforcement, the interface characteristics has great disparities with the two sides of interface. Material interfaces bonding is virtually atom bonding, depending on atoms arrangement and electron density distributions.

From the viewpoint of atom scale, if we understand the interface microstructure and the interface stability, we would grasp the relationship between the interface and material properties, thus take advantage of “interface engineering”[5] to develop the composites. CHENG[6] proposed the revised TFD (Thomas-Fermi-Dirac) model, the electron boundary condition is ascertained, namely electron density must be continuing among the atom bonding planes. This is determined by quantum condition of wave function continuity. Based on it, LIU et al[7] proposed a method to calculate the biphas interface valence electron structure, and found that the electron density of (111)_γ//(110)_α interface in steel is continuous[8]. This confirmed the existence of the above mentioned electron boundary condition. In this brief communication, emphasis will be made to study the interface electron structure between reinforcement TiC and Fe₃Al matrix, and to verify whether consistent crystallographic orientation relationships exist between TiC and Fe₃Al matrix. The valence electron structure (VES) of TiC ceramic phase and Fe₃Al intermetallic phase in TiC/Fe₃Al composite is calculated

with YU's EET.

2 VES calculation

2.1 VES of Fe₃Al and valence electron density

The DO₃ cell structure of Fe₃Al is shown in Fig.1, O_h⁵(m3m) type of space group. One DO₃ cell consists of four A2 (bcc) cells and four B2 cells, belongs to face centered cubic structure. Its lattice constant *a* is 0.578 nm. The Fe atoms located in the center of cell interior, or in the center of cell edge and the top of the cell are expressed as Fe^I. The Fe and Al atoms at the diagonal 1/4 and 3/4 of the cell interior are expressed as Fe^{II} and Al, respectively. Therefore the structure formula of Fe₃Al can be written as Fe^IFe₂^{II}Al. Only eight kinds of covalent bonds in DO₃ structure are considered. The experimented bond lengths (*D_{na}*) and equivalent bond numbers (*I_a*) are listed in in Table 1.

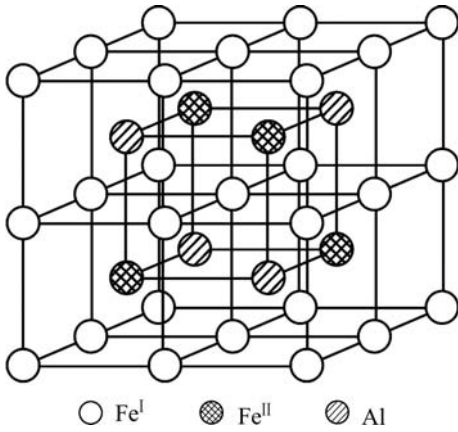


Fig.1 Unit cell of DO₃ structure Fe₃Al

Electron density of various crystallographic planes of Fe₃Al is calculated. The atoms on the (100) plane form only one kind of bond, i.e. $D_{n_C}^{Fe^{II}-Fe^{II}}$. The equivalent bond number in (100) plane is 4, the total covalent electrons on (100) crystal plane is $n_C^{(100)} = 4n_C$, and the area of (100) plane is

$$S_{(100)} = a^2$$

Thus the electron density of (100) crystal plane is

$$\rho_{(100)Fe_3Al} = \frac{4n_C}{a^2} \tag{1}$$

There are four kinds of bonds on (220) crystal planes, i.e. $D_{n_A}^{Fe^{II}-Al}$, $D_{n_B}^{Fe^{II}-Fe^I}$, $D_{n_C}^{Fe^{II}-Fe^{II}}$ and $D_{n_D}^{Fe^I-Al}$. The numbers of equivalent bond are 4, 4, 2, 2, respectively. Therefore, the total number of covalent electron on (220) plane is

$$\sum_{n_C}^{(220)} = 4n_A + 4n_B + 2n_C + 2n_D$$

Table 1 Experimental covalent bond distances and equivalent bondnumbers of binary Fe₃Al unit cell

Bond	<i>D_{na}</i> /nm	<i>I_a</i>
Fe ^{II} —Al(A)	$D_{nA} = \frac{\sqrt{3}}{4} a$	16
Fe ^{II} —Fe ^I (B)	$D_{nB} = \frac{\sqrt{3}}{4} a$	16
Fe ^{II} —Fe ^{II} (C)	$D_{nC} = \frac{1}{2} a$	12
Fe ^{II} —Al(D)	$D_{nD} = \frac{1}{2} a$	12
Al—Al(E)	$D_{nE} = \frac{\sqrt{2}}{2} a$	12
Fe ^I —Fe ^I (F)	$D_{nF} = \frac{\sqrt{2}}{2} a$	12
Fe ^{II} —Fe ^{II} (G)	$D_{nG} = \frac{\sqrt{2}}{2} a$	12
Fe ^{II} —Fe ^{II} (H)	$D_{nH} = \frac{\sqrt{3}}{2} a$	16

The area of the (220) crystal plane of Fe₃Al is

$$S_{(220)} = \sqrt{2} a^2$$

So the electron density of (220) crystal plane is

$$\rho_{(220)Fe_3Al} = \frac{4n_A + 4n_B + 2n_C + 2n_D}{\sqrt{2}a^2} \tag{2}$$

Fe^{II}, Fe^I and Al atoms arrange orderly on the (111) crystal plane, interatomic distances are the third near neighborhood, their covalent electron numbers are relatively scarce. Thus the electron density of (111) crystal plane can be neglected in first-class approximately.

According to the method of bond length difference(BLD)[9] in EET, the data in the binary hybridization list of Fe and the binary hybridization list of Al can be scanned using a computer so as to find all resolutions that satisfies the criterion of EET: $\Delta D_{na} < 0.005$ nm. The result shows there are 636(σ_N) kinds of resolutions. Here let σ_N represent the number of all probable groups of atom state. Substitute covalent electron numbers: *n_a* distributing the mentioned bonds into Eqns.(1) and (2). The electron density value scale of (100) and (220) crystal planes are 0.783 8–1.814 8 nm⁻², 6.475 8–8.969 8 nm⁻², respectively.

2.2 VES of TiC and valence electron density

TiC cell is B1 type of structure, Fm3m type of space group, as shown in Fig.2. Its lattice constant *a* is 0.216 45 nm. According to Ref.[10], only 4 kinds of covalent

bonds in B1 structure are considered which are precise enough for ordinary research. Their names, experimented bond lengths and equivalent bond numbers are as follows:

$$D_{nA}^{Ti-C} = a, I_A=6;$$

$$D_{nB}^{Ti-Ti} = \sqrt{2}a, I_B=6;$$

$$D_{nC}^{C-C} = \sqrt{2}a, I_C=6;$$

$$D_{nD}^{Ti-C} = \sqrt{3}a, I_D=8$$

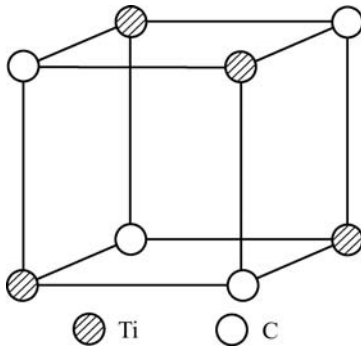


Fig.2 Unit cell of B1 structure TiC

There are three kinds of bonds distributing on the (100) crystal plane, namely D_{nA}^{Ti-C} , D_{nB}^{Ti-Ti} and D_{nC}^{C-C} . Their equivalent bond numbers are 4, 2, 2, respectively. The area of (100) crystal plane of TiC is

$$S_{(100)}=a^2$$

Therefore the electron density of its (100) crystal plane is

$$\rho_{(100)_{TiC}} = \frac{4n_A + 2n_B + 2n_C}{a^2} \quad (3)$$

But there are four kinds of bond distributing on (110) crystal plane, namely D_{nA}^{Ti-C} , D_{nB}^{Ti-Ti} , D_{nC}^{C-C} and D_{nD}^{Ti-C} . Their equivalent bond numbers are 2, 1, 1, 4, respectively. The area of the (110) crystal plane of TiC is

$$S_{(110)}=\sqrt{2}a^2$$

Therefore the electron density of its (110) crystal plane is

$$\rho_{(110)_{TiC}} = \frac{2n_A + n_B + n_C + 4n_D}{\sqrt{2}a^2} \quad (4)$$

Otherwise, only one kind of bond distributing on the (111) crystal plane, which is C—C bond with equivalent bond number of 3. The area of (111) crystal plane of TiC is

$$S_{(111)}=\frac{\sqrt{3}}{2}a^2$$

Thus the electron density of its (111) crystal plane is

$$\rho_{(111)_{TiC}} = \frac{3n_C}{\sqrt{3}/2a^2} = \frac{2\sqrt{3}n_C}{a^2} \quad (5)$$

According to Ref.[11], atom Ti is A-type hybridization. The results show that $\sigma_N=20$ resolutions satisfy the criterion of EET. The numbers of covalent electron of probable atom state are substituted into Eqns.(3), (4) and (5). The electron density value scale of (100), (110), (111) crystal planes are 34.039 9– 47.229 8 nm^{-2} , 0.755 3–1.048 1 nm^{-2} , 0.177–0.245 5 nm^{-2} , respectively.

3 VES of biphase interface

3.1 Continuous interface electron density of atom state groups

According to Liu's theory of interface valence electron structure, the interface electron density is defined as continuity in first-class approximately, namely $\Delta\rho < 10\%$ is regarded as continuity. However $\Delta\rho > 10\%$ is defined as deviation from continuity. These definitions are significant in material fields[12]. The relative covalent electron density difference between $TiC_{(uvw)}/Fe_3Al_{(hkl)}$ interfaces is

$$\Delta\rho = \frac{|\rho_{(uvw)_{Fe_3Al}} - \rho_{(hkl)_{TiC}}|}{\frac{1}{2}[\rho_{(uvw)_{Fe_3Al}} + \rho_{(hkl)_{TiC}}]} \quad (6)$$

According to the criterion: $\Delta\rho < 10\%$, the number of atom state groups λ which keeps continuous interface electron density can be counted.

The electron density of $(100)_{Fe_3Al}$ and $(110)_{TiC}$ can be scanned using a computer to find $\lambda=4\ 758$. Here, it is referred that the more λ is, the more stable the structure is when the condition changes[8].

3.2 Optimal states of interface electron density continuity

The atom states corresponding to the minimum value of electron density difference is listed in Table 2. As for $(100)_{Fe_3Al} // (110)_{TiC}$ interface, absolute value of minimum electron density difference along the interface is 0.007 37 nm^{-2} , and relative value is 0.759%. Here

$$\rho_{(110)_{TiC}} = 0.966\ 99\ \text{nm}^{-2}, \sigma_{Ti}=12, \sigma_C=5;$$

$$\rho_{(100)_{Fe_3Al}} = 0.974\ 36\ \text{nm}^{-2}, \sigma_{Fe^I}=11,$$

$$\sigma_{Fe^{II}} = 12, \sigma_{Al}=6$$

$$\Delta\rho_{(100)_{Fe_3Al} // (110)_{TiC}} = 0.759\%$$

Table 2 TiC₍₁₁₀₎/Fe₃Al₍₁₀₀₎ interface valence electron structure

Bond	I_a	D_{na}/nm	\bar{D}_{na}/nm	n_a	$\Delta D_{na}/\text{pm}$
$D_{nA}^{\text{Fe}^{\text{II}}-\text{Al}}$	16	0.250 28	0.252 23	0.456 38	1.95
$D_{nB}^{\text{Fe}^{\text{II}}-\text{Fe}^{\text{I}}}$	16	0.250 28	0.252 23	0.368 55	1.95
$D_{nC}^{\text{Fe}^{\text{II}}-\text{Fe}^{\text{II}}}$	12	0.289 00	0.290 95	0.081 38	1.95
$D_{nD}^{\text{Fe}^{\text{I}}-\text{Al}}$	12	0.289 00	0.290 95	0.105 48	1.95
$D_{nE}^{\text{Al}-\text{Al}}$	12	0.408 71	0.410 65	0.001 32	1.95
$D_{nF}^{\text{Fe}^{\text{I}}-\text{Fe}^{\text{I}}}$	12	0.408 71	0.410 65	0.000 86	1.95
$D_{nG}^{\text{Fe}^{\text{II}}-\text{Fe}^{\text{II}}}$	12	0.408 71	0.410 65	0.000 82	1.95
$D_{nH}^{\text{Fe}^{\text{II}}-\text{Fe}^{\text{II}}}$	16	0.500 56	0.502 51	0.000 02	1.95
$D_{nA}^{\text{Ti}-\text{C}}$	6	0.216 45	0.219 65	0.464	3.14
$D_{nB}^{\text{Ti}-\text{Ti}}$	6	0.306 11	0.309 25	0.090 31	3.14
$D_{nC}^{\text{C}-\text{C}}$	6	0.306 11	0.308 89	0.002 45	3.14
$D_{nD}^{\text{Ti}-\text{C}}$	8	0.374 90	0.378 05	0.001 06	3.14

$A=4.758$; $\Delta\rho=0.759\%$. VES corresponding to minimum value of electron density: Fe₃Al: $S=0.334\ 084\ \text{nm}^2$, $\Sigma n_C=15.477\ 64$, $\rho=0.974\ 36\ \text{nm}^2$, $\sigma_N=636$;

TiC: $S=0.066\ 26\ \text{nm}^2$, $\Sigma n_C=3.349\ 036$, $\rho=0.966\ 99\ \text{nm}^2$, $\sigma_N=20$

Al: $R(1)=0.119\ \text{nm}$, $n_C=3$; Fe^I: $R(1)=0.113\ 43\ \text{nm}$, $n_C=4.002\ 1$; Fe^{II}: $R(1)=0.112\ 79\ \text{nm}$, $n_C=4.240$;

C: $R(1)=0.076\ 3\ \text{nm}$, $n_C=3.904$; Ti: $R(1)=0.123\ 3\ \text{nm}$, $n_C=2.795$.

However, as for TiC, the atom stable states are: Ti atom is at the 13th level of A-type hybridization, and C atom is at the 6th hybrid level. Meantime the electron density of (110) crystal plane is $1.016\ 5\ \text{nm}^{-2}$. With regard to Fe₃Al, atom stable states are: Fe^I and Fe^{II} are at the 11th level and the 14th level of B-type hybridization, respectively. Al is at the 3rd hybrid level. Meantime the electron density of (100) crystal plane is $0.874\ 7\ \text{nm}^{-2}$. That is to say when TiC phase and Fe₃Al phase are the most stable state, the biphasic interface electron density deviates from continuity, the percentage value of minimum electron density difference along the interface is 15%. So the atom state, which keeps the electron density continuous, is a series of atomic excited-state.

Additionally, Al atom is at 6th level compared with the 2nd level of the document[13]. In composites, Al will supply more covalent electrons to form bond, result in fraction of covalent bond increasing in iron aluminides. Thus coherent or semi-coherent interface may be formed between iron aluminides phase and titanium carbide phase leading to strengthen the interface.

4 Composite materials fabrication techniques

Fe₃Al/TiC composites can be fabricated by mechanical alloying processing and in-situ processing techniques. With regard to the former, the pre-mixed powder was processed by mechanical alloying followed by hot pressure sintering. Simple mixed powders undergo the formation of intermediate phases, it will have influence on the interface bonding. In contrast to

mechanical alloying processing, an in-situ processing techniques[14] during composite fabrication have a potential for good mechanical properties because the interface between the matrix and reinforcement may have a good bonding strength due to the avoidance of contamination by oxidation and other detrimental surface reaction.

The large TiC particles tend to precipitate from the melt with the shape of cuboidal, spherical, starlike and dendritic crystal due to the growth environmental diversities. Formation mechanism of the cuboidal shape TiC in the liquid iron-aluminide alloy is not clear at present[13]. Additionally, it is also found that increased titanium and carbon contents do not increase the size of large particles. One possible explanation[12] is that this phenomenon may result from the difference in the interfacial free energy between different phases. If surface energy between TiC particles with different orientations is larger than two times that between liquid iron-aluminum alloy and TiC particle, TiC particles will not agglomerate. Some studies[15, 16] also show that cuboidal TiC particles with (100) facets precipitate in iron melt by in-situ processing. However, 12-faced polyhedron TiC particles were reported to form in aluminum melt by in-situ processing.

When TiC particle bonds with metallic phase, the crystal will grow along the specified crystallographic orientation of hard core. But the crystallographic orientation relation is not determined exclusively. From Table 2 it can be found that (110)_{TiC}//(100)_{FeAl} interface has continuous interface electron density and relatively small $\Delta\rho_{\text{min}}$. This result just confirms the fact that TiC particles grow on the non-close-packed plane, the final

shape is cuboidal. (110)_{TiC}//(100)_{FeAl} crystallographic orientation relationship is believed to the formation mechanism of the cuboidal shape of TiC.

Otherwise, the results show the maximum electron density of (100)_{TiC} deviates from continuity with the arbitrary crystal plane of Fe₃Al. From the viewpoint of CHENG-LIU theory, crystal particle growth is accompanied by the electrons transporting, the electron density deviation from continuity can lead to constraint the particle growth. It is well explained that the increased titanium and carbon contents do not increase the size of large particles.

5 Conclusions

1) B1 structure of TiC has 20 probable states of Ti atom and C atom, D0₃ structure of Fe₃Al has 636 probable states of Fe atom and Al atom.

2) (110)_{TiC}//(100)_{FeAl} interface has continuous interface electron density; the number of atom state groups $\lambda=475.8$. Absolute value of minimum electron density difference along the interface is 0.00737 nm^{-2} , and relative value is 0.759%. Here

$$\rho_{(110)_{\text{TiC}}} = 0.96699 \text{ nm}^{-2}, \rho_{(100)_{\text{Fe}_3\text{Al}}} = 0.97436 \text{ nm}^{-2}.$$

Atomic state is: Ti is at the 12th level of A-type hybridization, and C is at the 5th hybrid level. Fe^I and Fe^{II} are at the 11th level and the 12th level of B-type hybridization, respectively; Al is at the 6th hybrid level.

3) From the viewpoint of the continuity and deviation from continuity of interface electron density, it is well explained that the formation mechanism of cuboidal shape of TiC particle and the micromechanisms of small size of TiC particle. This method of investigating the biphasic interface is heuristic for other intermetallic matrix composites.

Reference

[1] TANG Wen-ming, TANG Hong-jun, ZHENG Zhi-xiang, WU

- Yu-cheng, DONG Ji-ling. Progresses in studies on Fe-Al intermetallic matrix composites [J]. Trans Nonferrous Met Soc China, 2003, 13(4): 811–813.
- [2] SCHNEIBEL J H, CARMICHAEL C A, SPECHT E D, SUBRAMANIAN R. Liquid-phase sintered iron aluminide-ceramic composites [J]. Intermetallics, 1997, 5(1): 61–67.
- [3] ALMAN D E, TYLCZAK J H, HAWK J A, SCHNEIBEL J H. An assessment of the erosion resistance of iron-aluminide cermets at room and elevated temperatures [J]. Mater Sci Eng A, 2002, A329–331: 602–608.
- [4] SUNDAR R S, BALIGIDAD R G, PRASAD D H, SASTRY D H. Processing of iron aluminides [J]. Mater Sci Eng A, 1998, A258(1–2): 219–228.
- [5] YE Heng-qiang. Material Interfaces Structure and Properties [M]. Beijing: Science Press, 1999. 254.(in Chinese)
- [6] CHENG Kai-jia. Application of TFD model and Yu's theory to material design [J]. Progress in Nature Science, 1993, 3(5): 211–230.
- [7] LIU Zhi-lin, LI Zhi-lin, LIU Wei-dong. Interface Electron Structure and Interface Properties [M]. Beijing: Science Press, 2002. 85.(in Chinese)
- [8] LIU Zhi-lin, LI Zhi-lin, SUN Zhen-guo. Electron density of austenite/martensite biphasic interface [J]. Chinese Science Bulletin, 1996, 41(5): 367.(in Chinese)
- [9] ZHANG Rui-lin. The Empirical Electron Theory of Solids and Molecules [M]. Changchun: Jilin Science and Technology Press, 1993. 83.(in Chinese)
- [10] FUN Run-hua, YIN Yan-sheng, SUN Jia-tao, WANG Xin, CHEN Shou-gang. FeAl/TiC composite interface electron structure [J]. Progress in Nature Science, 2004, 14(3): 307–311.(in Chinese)
- [11] WANG Huan-rong, YE Yi-fu, MIN Guang-hui. TiC valence electron structure and analysis of properties [J]. Chinese Science Bulletin, 2001, 46(3): 58–63.(in Chinese)
- [12] SUN Zhen-guo, LI Zhi-lin, LIU Zhi-lin. Calculation of biphasic interface electron density in alloy [J]. Chinese Science Bulletin, 1995, 40(24): 2219–2222.(in Chinese)
- [13] SUN Kang-ning, YIN Yan-sheng, LI Ai-min. Intermetallics/Ceramics Matrix Composites [M]. Beijing: China Machine Industry Press, 2002. 82–84.(in Chinese)
- [14] KO S H, HANADA S. In-situ production and microstructures of iron aluminide/TiC composites [J]. Intermetallics, 1999, 7(8): 953–955.
- [15] KO S H, PARK B G, HASHIMOTO H, ABE T, PARK Y H. Effect of MA on microstructure and synthesis path of in-situ TiC reinforced Fe–28at%Al intermetallic composites [J]. Mater Sci Eng A, 2002, A329–331: 78–83.
- [16] KRASNOWSKI M, WITEK A, KULIK T. The FeAl-30%TiC nanocomposite produced by mechanical alloying and hot-pressing consolidation [J]. Intermetallics, 2002, 10(4): 373–375.

(Edited by LONG Huai-zhong)